

Exponential time differencing for matrix-valued dynamical systems*

Nayef Shkeir

Mathematics Institute, University of Warwick, Coventry, CV4 7AL, United Kingdom

Tobias Schäfer

Department of Mathematics, College of Staten Island, CUNY, NY 1S-215, USA

Tobias Grafke

Mathematics Institute, University of Warwick, Coventry, CV4 7AL, United Kingdom

June 21, 2024

Abstract

Matrix evolution equations occur in many applications, such as dynamical Lyapunov/Sylvester systems or Riccati equations in optimization and stochastic control, machine learning or data assimilation. In many cases, their tightest stability condition is coming from a linear term. Exponential time differencing (ETD) is known to produce highly stable numerical schemes by treating the linear term in an exact fashion. In particular, for stiff problems, ETD methods are a method of choice. We propose an extension of the class of ETD algorithms to matrix-valued dynamical equations. This allows us to produce highly efficient and stable integration schemes. We show their efficiency and applicability for a variety of real-world problems, from geophysical applications to dynamical problems in machine learning.

1 Introduction

Matrix-valued dynamical systems play a crucial role in understanding complex phenomena in the sciences. They often occur as differential Lyapunov, differential Sylvester or matrix-Riccati equations in the context of optimization, but are also present in stochastic control

*This work was supported by the Engineering and Physical Sciences Research Council (EPSRC) through the Mathematics of Systems II Centre for Doctoral Training at the University of Warwick (reference EP/S022244/1). T.G. acknowledges the support received from the EPSRC projects EP/T011866/1 and EP/V013319/1. The work of T.S. was supported by the NSF grant DMS-2012548. For the purpose of open access, the author has applied a Creative Commons Attribution (CC BY) licence to any Author Accepted Manuscript version arising from this submission.

and data assimilation. Differential Lyapunov equations appear in stability analysis for continuous linear time-varying systems [1] where analysis and controllability depend on the solutions of the Lyapunov equations. Differential Lyapunov/Sylvester equations also have important applications in optimal control [2], model reduction [3] and machine learning [4]. Matrix-Riccati equations play a significant role in the context of continuous-time Kalman filters, which are widely utilized in numerous scientific and engineering disciplines for state estimation and control of dynamical systems [5, 6].

Matrix-valued dynamical equations usually come with tight stability constraints, for example, because of the presence of high-order linear differential operators (e.g. diffusion or (hyper-)viscosity), or poor conditioning in the (quasi-)linear dynamics [7, 8]. Moreover, many real-world systems have multiple time scales or are oscillatory, making the system stiff [9]. For systems with scale separation, semi-Lagrangian methods have been popular in physics applications [10].

There has been some effort to solve matrix-valued dynamical systems numerically, such as backward differentiation formula (BDF) methods [11], Parareal based algorithms [12] and Krylov subspace methods [13, 14]. There has also been some preliminary work on the use of exponential integrators for Matrix-Riccati equations [15]. However, many of these approaches are infeasible for large and stiff Matrix-valued systems.

For scalar systems, exponential time differencing (ETD) methods provide accurate numerical solutions to stiff dynamical problems [16, 17] and have been applied to a variety of problems involving dynamical systems modeled by ordinary and partial differential evolution equations [18, 19, 20, 21, 22]. These schemes have been shown to be especially suited to quasi-linear systems which can be split into a linear part that contains much of the stiffness of the dynamics and a non-linear part [23, 19].

Given these two developments, it is natural to ask if ETD methods can be extended to matrix-valued evolution equations by making use of the particular structure present in such problems. The main objective of this present work is to present a method of how to generalize ETD schemes to matrix-valued problems. Similar to the case of standard scalar ETD problems, it turns out that the key idea of the approach, namely to integrate the linear part of the problem exactly, can be carried over to matrix-valued problems. The remaining nonlinear integral term, however, must be treated with more care than in the scalar case, since non-commutativity gives rise to complications, leading to additional terms in the numerical scheme.

The structure of this paper is as follows: We first review the basic idea of ETD algorithms in their extension to matrix-valued equations. A particular focus are commutator relations that make the study of ETD algorithms in the matrix case fundamentally different to the scalar case. We then introduce a first-order matrix-ETD scheme, and two second-order algorithms, a matrix-ETD multistep scheme and a matrix-ETD Runge-Kutta scheme. After the theoretical analysis, we illustrate these novel methods in a variety of examples. In the last section of the paper, we discuss a more complicated application stemming from continuous graph neural networks. This problem is different from the previous ones in the sense that it involves (a) non-square matrices and (b) lacks certain commutation relations. We show how both these difficulties can be overcome and the previously developed methods can be adapted to this case as well. All schemes derived in this paper are explicit schemes.

2 Matrix Exponential Time Differencing

Let us consider a matrix evolution equation for $Q(t) \in \mathbb{R}^{n \times n}$ given by

$$\dot{Q} = LQ + QR + N(Q, t), \quad Q(0) = Q_0, \quad (1)$$

with linear operators $L, R \in \mathbb{R}^{n \times n}$ multiplied once from the left and from the right, respectively, against Q , and with $N(Q, t) : \mathbb{R}^{n \times n} \times [0, T] \rightarrow \mathbb{R}^{n \times n}$ being potentially nonlinear. Note that, in what follows, we define the commutator $[A, B] := AB - BA$ for $A, B \in \mathbb{R}^{n \times n}$ as usual. It is also important to note that the linear operators (L and R) are in the same space as the unknown Q .

The first step toward a solution of the problem (1) is to solve the linear problem. In the scalar case, this is obtained by using an integrating factor. In the matrix case at hand, we can multiply Q from the left by e^{-tL} and right by e^{-tR} and differentiate to obtain

$$\begin{aligned} \frac{d}{dt} (e^{-tL} Q e^{-tR}) &= e^{-tL} \dot{Q} e^{-tR} - e^{-tL} L Q e^{-tR} - e^{-tL} Q R e^{-tR} \\ &= e^{-tL} N(Q, t) e^{-tR}, \end{aligned}$$

an equation we can directly integrate. Here e^A for $A \in \mathbb{R}^{n \times n}$ is the matrix exponential. The solution of (1) in the time interval $[t_n, t_{n+1}]$ where $t_{n+1} = t_n + \Delta t$ and $t_0 = 0$, is given by the variation-of-constants formula

$$Q(t_{n+1}) = e^{\Delta t L} Q(t_n) e^{\Delta t R} + \int_0^{\Delta t} e^{(\Delta t - \tau)L} N(t_n + \tau) e^{(\Delta t - \tau)R} d\tau, \quad (2)$$

where we need to evaluate the integral in (2), which, if the commutator $[N, e^{sR}]$ is non-zero, is not trivial (equally if $[N, e^{sL}] \neq 0$). With classic ETD methods, we try to approximate the nonlinear term in the integral using an algebraic polynomial. For now, we consider the case $[L, R] = 0$. Note that many (but not all) problems of practical relevance satisfy this condition (a common case is e.g. $R = L^T$ and L normal). Throughout this paper, we adopt the notation $N(Q(t_n), t_n) = N(t_n)$ for simplicity.

We also define φ functions commonly seen in the exponential integrators literature [24, 25] to simplify notation. Let $\theta = \tau/\Delta t \in [0, 1]$ and we then define these functions as

$$\varphi_k(A) = \int_0^1 e^{(1-\theta)A} \frac{\theta^{k-1}}{(k-1)!} d\theta, \quad k \geq 1, \quad (3)$$

with $\varphi_0(A) = e^{\Delta t A}$ for some matrix $A \in \mathbb{R}^{n \times n}$. We also note that

$$\varphi_{k+1}(A) = A^{-1}[\varphi_k(A) - \varphi_k(0)], \quad \varphi_k(0) = \frac{1}{k!}. \quad (4)$$

For most of the numerical examples we present in this paper, we can compute our φ functions directly and in cases where A is ill-conditioned, we introduce regularization. There is a breadth of literature on computing the φ functions efficiently such as Krylov subspace methods [26] and the Padé method with the scaling and squaring strategy [27].

2.1 Commutator series

We can multiply the commutator $[N, e^{sR}]$ from the left by e^{sL}

$$e^{sL}[N, e^{sR}] = e^{sL}N e^{sR} - e^{s(L+R)}N,$$

where $e^L e^R = e^{L+R}$ only because we demand commutativity. This means we can rewrite our integral in (2) as

$$\begin{aligned} \int_0^{\Delta t} e^{(\Delta t - \tau)L} N(t_n + \tau) e^{(\Delta t - \tau)R} d\tau &= \int_0^{\Delta t} e^{(\Delta t - \tau)(L+R)} N(t_n + \tau) d\tau \\ &+ \int_0^{\Delta t} e^{(\Delta t - \tau)L} [N(t_n + \tau), e^{(\Delta t - \tau)R}] d\tau. \end{aligned} \quad (5)$$

We can derive numerical schemes via a truncation of the commutator by considering the power expansion

$$e^{sR} = \sum_{k=0}^{\infty} \frac{s^k}{k!} R^k,$$

which gives us the commutator series expansion

$$[N, e^{sR}] = \sum_{k=0}^{\infty} \frac{s^k}{k!} [N, R^k] = s[N, R] + \frac{1}{2}s^2[N, R^2] + \dots$$

Our goal is to approximate the integral up to a certain order and considering that $s \in [0, \Delta t]$, truncating the commutator series at a certain order of s will allow us to carry out this expansion.

2.2 First order Matrix Exponential Time Differencing Scheme, METD1

With all the building blocks in place, we can quickly arrive at the first order scheme, using

$$\begin{aligned} \int_0^{\Delta t} e^{(\Delta t - \tau)L} N(t_n + \tau) e^{(\Delta t - \tau)R} d\tau &= \Delta t \int_0^1 e^{(1-\theta)\Delta t(L+R)} N(t_n + \Delta t\theta) d\theta \\ &+ \Delta t^2 \int_0^1 (1-\theta) e^{(1-\theta)\Delta tL} [N(t_n + \Delta t\theta), R] d\theta \\ &+ \mathcal{O}(\Delta t^3) \\ &\approx \Delta t \int_0^1 e^{(1-\theta)\Delta t(L+R)} d\theta N(t_n) \\ &= (L+R)^{-1} (e^{\Delta t(L+R)} - \mathbf{1}) N(t_n), \end{aligned} \quad (6)$$

where we approximate N to first order as a constant between t_n and t_{n+1} (in the following, index n represents the temporal index for discrete time steps). At this point, we need to require the sum $L+R$ to be non-singular. Details of the computation of the integral are given in A.1. The commutator integral in (6) is $\mathcal{O}(\Delta t^2)$ which justifies dropping the commutator integral for the METD1 scheme.

Summarizing these calculations, we have obtained a first order METD scheme as

$$Q_{n+1} = \varphi_0(\Delta t L) Q_n \varphi_0(\Delta t R) + \Delta t \varphi_1(\Delta t(L+R)) N(Q_n, t_n), \quad (7)$$

where by solving the corresponding integrals in (3), we have

$$\begin{aligned} \varphi_0(\Delta t A) &= e^{\Delta t A}, \\ \varphi_1(\Delta t A) &= (\Delta t A)^{-1} [e^{\Delta t A} - \mathbf{1}]. \end{aligned}$$

2.3 Second order Multistep scheme, METD2

In order to derive a second-order scheme, we proceed similarly to the scalar case [16] and now approximate the nonlinear term as

$$N(t_n + \tau) = N_n + \tau(N_n - N_{n-1})/\Delta t + \mathcal{O}(\Delta t^2),$$

which is a first order polynomial in τ , where τ is in the interval $0 \leq \tau \leq \Delta t$. We carry out the same steps as for the first order scheme, but now have to consider the commutator expansion in the integral in (5). Setting the backward difference ∇N_n defined as $\nabla N_n = N_n - N_{n-1}$, we arrive at the following integrals

$$\begin{aligned} \int_0^{\Delta t} e^{(\Delta t - \tau)L} N(t_n + \tau) e^{(\Delta t - \tau)R} d\tau &= \Delta t \int_0^1 e^{(1-\theta)\Delta t(L+R)} N(t_n + \Delta t\theta) d\theta \\ &\quad + \Delta t^2 \int_0^1 (1-\theta) e^{(1-\theta)\Delta t L} [N(t_n + \Delta t\theta), R] d\theta \\ &\quad + \mathcal{O}(\Delta t^3) \\ &\approx \Delta t \int_0^1 e^{(1-\theta)\Delta t(L+R)} (N_n + \theta \nabla N_n) d\theta \\ &\quad + \Delta t^2 \int_0^1 (1-\theta) e^{(1-\theta)\Delta t L} [(N_n + \theta \nabla N_n), R] d\theta \end{aligned} \quad (8)$$

to second order. We treat these integrals in detail in A.2. Putting everything together, we obtain the METD2 scheme as

$$\begin{aligned} Q_{n+1} &= \varphi_0(\Delta t L) Q_n \varphi_0(\Delta t R) + \Delta t \varphi_1(\Delta t(L+R)) N_n + \\ &\quad \Delta t \varphi_2(\Delta t(L+R)) \nabla N_n + \Delta t^2 (\varphi_1(\Delta t L) - \varphi_2(\Delta t L)) [N_n, R] + \\ &\quad \Delta t^2 (\varphi_2(\Delta t L) - \varphi_3(\Delta t L)) [\nabla N_n, R], \end{aligned}$$

where by solving the corresponding integrals in (3), we have

$$\begin{aligned} \varphi_0(A) &= e^{\Delta t A}, & \varphi_1(A) &= (\Delta t A)^{-1} [e^{\Delta t A} - \mathbf{1}], \\ \varphi_2(A) &= (\Delta t A)^{-2} [e^{\Delta t A} - \Delta t A - \mathbf{1}], \\ \varphi_3(A) &= (\Delta t A)^{-3} [\Delta t L + \Delta t e^{\Delta t L} L - 2e^{\Delta t L} + 2\mathbf{1}]. \end{aligned}$$

2.4 Second order Runge-Kutta scheme, METD2RK

Multistep methods can be inconvenient to implement with only one initial value. Runge-Kutta (RK) methods avoid this problem, and further often have larger stability regions and smaller error constants compared to multistep methods. This comes at the price of a larger number of evaluations of the RHS per step. For a second order RK method, we take an intermediate step given by

$$A_n = \varphi_0(\Delta t L) Q_n \varphi_0(\Delta t R) + \Delta t \varphi_1(\Delta t(L + R)) N(Q_n, t_n),$$

which is just the first order scheme (7). For the METD2RK scheme, we take the second order approximation of the non-linear term and consider

$$N(t_n + \tau) = N(Q_n, t_n) + \tau(N(A_n, t_n + \Delta t) - N(Q_n, t_n))/\Delta t + \mathcal{O}(\Delta t^2),$$

which combining with (8) gives us the ETD2RK scheme as

$$\begin{aligned} Q_{n+1} = & A_n + \Delta t \varphi_2(\Delta t(L + R))(N(A_n, t_n + \Delta t) - N(Q_n, t_n)) \\ & + \Delta t^2 (\varphi_1(\Delta t L) - \varphi_2(\Delta t L)) [N(Q_n, t_n), R] \\ & + \Delta t^2 (\varphi_2(\Delta t L) - \varphi_3(\Delta t L)) [(N(A_n, t_n + \Delta t) - N(Q_n, t_n)), R]. \end{aligned}$$

3 Error analysis

Before the subsequent analysis, we adopt the following definition

Definition 1 Let \mathcal{B} be a Banach algebra, i.e., a triple $(\mathcal{B}, *, \|\cdot\|)$ where $(\mathcal{B}, *)$ is a unital associative algebra, and $(\mathcal{B}, \|\cdot\|)$ is a (real or complex) Banach space, where the norm $\|\cdot\|$ is compatible with the multiplication $\|x * y\| \leq \|x\| \|y\|$ for any $x, y \in \mathcal{B}$. The commutator is then defined as $[x, y] = x * y - y * x$.

In practise, we discretise our domain such that we will have \mathcal{B} being the space of real (or complex) $n \times n$ matrices. We also make the following assumptions

Assumption 1 We assume that $L, R \in \mathcal{B}$ are bounded linear operators. Further, we assume that L is an infinitesimal generator of an analytic semigroup e^{tL} and the same for R and $L + R$.

This assumption implies that there exists constants $C > 0$ and $\omega \in \mathbb{R}$ such that

$$\|e^{tL}\| \leq C e^{\omega t}, \quad t \geq 0. \quad (9)$$

In particular, we have that φ_k in (3) for $k \geq 1$ are bounded operators.

Assumption 2 We assume that the nonlinearity $N : \mathcal{B} \times [0, T] \rightarrow \mathcal{B}$ is globally Lipschitz continuous on a strip along the exact solution. We have that N and the derivatives of N are uniformly bounded.

3.1 METD1 error analysis

To show the scaling of the truncation error for METD1, we first insert the exact solution, $Q(t_n)$, into our METD1 numerical scheme, which yields

$$Q(t_{n+1}) = \varphi_0(\Delta t L) Q(t_n) \varphi_0(\Delta t R) + \varphi_1(\Delta t(L + R)) N(Q(t_n), t_n) + \delta_{n+1}, \quad (10)$$

where δ_{n+1} is the defect. We can expand the non-linear term $N(t_n + \tau)$ in the integral in the variation-of-constants formula (2) using a Taylor expansion with an integral remainder as

$$N(t_n + \tau) = N(t_n) + \tau N'(t_n) + \int_0^\tau (\tau - \phi) N''(t_n + \phi) d\phi. \quad (11)$$

By comparing (10) and (2), we find that the defect is given by

$$\begin{aligned} \delta_{n+1} &= \Delta t^2 \varphi_2(\Delta t(L + R)) N'(t_n) \\ &\quad - \int_0^{\Delta t} e^{(\Delta t - \tau)L} \left[\int_0^\tau (\tau - \phi) N''(t_n + \phi) d\phi \right] e^{(\Delta t - \tau)R} d\tau \\ &\quad + \Delta t^2 (\varphi_1(\Delta t L) - \varphi_2(\Delta t L)) [N(t_n), R] \\ &\quad + \Delta t^2 (\varphi_1(\Delta t L) - \varphi_2(\Delta t L)) \left[\int_0^\tau N'(t_n + \phi) d\phi, R \right]. \end{aligned} \quad (12)$$

where the commutator terms come from the integral expansion in (6) by considering a Taylor expansion with an integral remainder to first order. We can see that the coefficients of $N''(t_n)$ are $O(\Delta t^3)$ and the term involving a commutator with $N'(t_n)$ is also $O(\Delta t^3)$. We can then bound our defect using assumptions 1 and 2 as

$$\begin{aligned} \|\delta_{n+1}\| &\leq C \left(\Delta t^2 K_1 + \Delta t^3 K_2 + \Delta t^2 \| [N(t_n), R] \| + \Delta t^2 \left\| \left[\int_0^\tau N'(t_n + \phi) d\phi, R \right] \right\| \right) \\ &\leq C \left(\Delta t^2 K_1 + \Delta t^3 K_2 + \Delta t^2 2 \| N(t_n) \| \| R \| + \Delta t^2 2 \left\| \int_0^\tau N'(t_n + \phi) d\phi \right\| \| R \| \right) \\ &= C \left(\Delta t^2 K_1 + \Delta t^3 K_2 + 2 \Delta t^2 K_0 M_R + 2 \Delta t^3 K_1 M_R \right) \end{aligned} \quad (13)$$

for a constant $C > 0$ where $K_j = \sup_{0 \leq t \leq t_{n+1}} \| N^{(j)}(t) \|$ where j indicates the derivative and $\| R \| = M_R$ since R is a bounded linear operator. From (13), we have that our METD1 scheme has local truncation error of $O(\Delta t^2)$.

3.2 METD2 local error

We now aim to show that the METD2 local truncation error is of $O(\Delta t^3)$. We insert the exact solution into the METD2 numerical scheme which yields

$$\begin{aligned} Q(t_{n+1}) &= \varphi_0(\Delta t L) Q(t_n) \varphi_0(\Delta t R) + \Delta t \varphi_1(\Delta t(L + R)) N(Q_n, t_n) + \\ &\quad \Delta t \varphi_2(\Delta t(L + R)) \xi(t_n) + \Delta t^2 (\varphi_1(\Delta t L) - \varphi_2(\Delta t L)) [N(Q_n, t_n), R] + \\ &\quad \Delta t^2 (\varphi_2(\Delta t L) - \varphi_3(\Delta t L)) [\xi(t_n), R] + \delta_{n+1}, \end{aligned}$$

with defect δ_{n+1} and $\xi(t_n) = N(Q(t_n), t_n) - N(Q(t_{n-1}), t_{n-1})$. Since the METD2 scheme depends on the current and previous timestep (as it is a multi-step scheme), we consider the interpolation error of the non-linearity for intermediate times $\eta(\theta) \in [t_{n-1}, t_{n+1}]$ as

$$N(t_n + \theta\Delta t) = N_n + \theta \nabla N_n + \frac{1}{2} \Delta t^2 \theta(\theta + 1) N''(\eta(\theta)) \quad (14)$$

where $\theta = \tau/\Delta t \in [0, 1]$ and ∇N_n is the backward difference defined as $\nabla N_n = N_n - N_{n-1}$. By the variation-of-constants formula (2), the defect is given by

$$\begin{aligned} \delta_{n+1} = & \frac{1}{2} \Delta t^3 \int_0^1 e^{(1-\theta)\Delta t L} \theta(\theta + 1) N''(\eta(\theta)) e^{(1-\theta)\Delta t R} d\theta \\ & + \Delta t^3 \int_0^1 (1-\theta)^2 e^{(1-\theta)\Delta t L} d\theta [N(t_n), R^2], \end{aligned} \quad (15)$$

where the second term comes from the the integral expansion in (6). Using assumptions 1 and 2, we can bound our defect by

$$\begin{aligned} \|\delta_{n+1}\| & \leq C \left(\Delta t^3 K_2 + \Delta t^3 \| [N(t_n), R^2] \| \right) \\ & \leq C \left(\Delta t^3 K_2 + 2\Delta t^3 K_0 M_R^2 \right), \end{aligned} \quad (16)$$

where we used the property $\|R^n\| \leq \|R\|^n$ of definition 1.

The error analysis for the METD2RK scheme can be performed similarly.

4 Numerical Examples

In this section, we compute and test the METD schemes with differential Lyapunov, Ricatti and Sylvester equations. Our main goal is to confirm the global truncation error of the schemes and show that it is applicable to real-world high dimensional complex systems from PDEs to machine learning. We start with simple tests and gradually increase complexity and generality.

4.1 A low-dimensional Lyapunov equation

As the simplest non-trivial example of a matrix evolution equation, we consider a Lyapunov system

$$\dot{C}(t) = AC(t) + C(t)A^T + \Sigma, \quad (17)$$

where $C(t) \in \mathbb{R}^{n \times n}$, $\Sigma \in \mathbb{R}^{n \times n}$ symmetric positive definite, and $A \in \mathbb{R}^{n \times n}$ normal ($AA^T = A^T A$) and negative definite. While this example is merely affine-linear, with $N = \Sigma$ independent of $C(t)$, it is still the case that the commutator is non-zero, $[N, L] \neq 0$. Due to N being constant in time, we do not have to use the second order approximation of the non-linear term ($\nabla N_n = 0$ in (8)). As a result of this, we can study the commutator series truncation. We solve the system (17) until time $t = 10$, where it is close enough to the solution C_∞ of the stationary Lyapunov equation that we can take $\|C(t) - C_\infty\|$ as the error. Solving this system for $n = 2$, from figure 1, we see that the first order METD1 scheme is indeed first order as its error is scaling like $\mathcal{O}(\Delta t)$, while METD2 is second order as it scales like

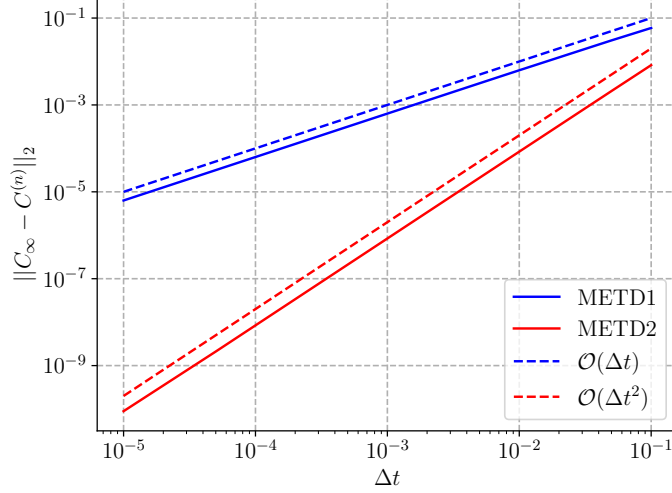


Figure 1: Difference between $C(t=10)$, solution to the dynamical Lyapunov equation (17), and the stationary solution C_∞ . The METD schemes solve the equation at their respective order.

$\mathcal{O}(\Delta t^2)$. In this simple example, the METD2RK scheme reduces to the METD2 scheme as a result of the constant nonlinear term. Note that numerically, these schemes have a computational complexity of $\mathcal{O}(n^3)$ since the main computational cost is dominated by the matrix exponential computation.

We next consider a system where the nonlinear term is truly nonlinear.

4.2 Continuous Time Algebraic Riccati equation

Another very frequent occurrence of matrix evolution equations is the dynamical continuous time algebraic Riccati equation (CARE), which appears for example in optimal control [28]. In contrast to the Lyapunov equation discussed above, here the nonlinear term is no longer merely a constant, but instead depends (quadratically) on the unknown. We consider an ODE for $X(t) \in \mathbb{R}^{n \times n}$ given by

$$\dot{X}(t) = X(t)L + L^T X(t) - X(t)DX(t) + Q, \quad (18)$$

where $L, D, C \in \mathbb{R}^{n \times n}$ and L normal, Q and D symmetric. As the simplest non-trivial example, we take $n = 2$ with

$$L = \begin{bmatrix} -2 & -2 \\ 2 & -2 \end{bmatrix}, \quad Q = \begin{bmatrix} 2 & 0 \\ 0 & 2 \end{bmatrix},$$

so that L is normal and Q is symmetric. Additionally, D is chosen to be symmetric but random,

$$D = BB^T \text{ where } (B)_{ij} \sim \mathcal{N}(0, 1).$$

The initial condition $X(0)$ is chosen to be a random matrix with each element of the matrix drawn from a normal distribution as well. While the solution to the dynamical Riccati

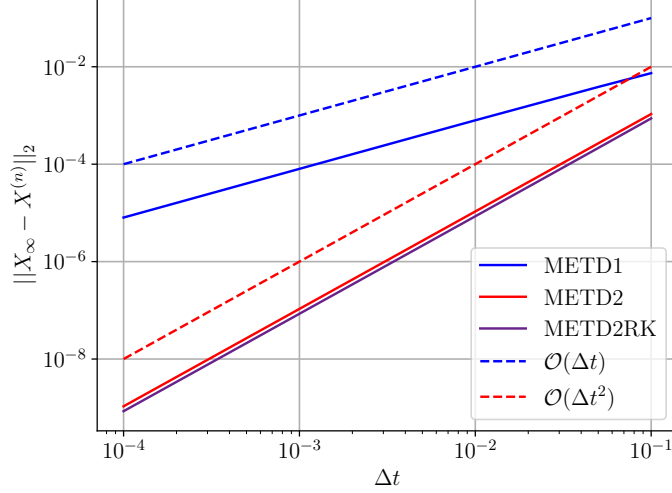


Figure 2: Difference between $X(t=100)$, solution to equation (18), and the stationary CARE solution X_∞ , for different values of Δt . The METD schemes approximate the stationary solution at their respective order.

equation (18) evolves continuously in time, we can compare the numerical accuracy of the METD schemes against the long-time solution, $t \rightarrow \infty$, where it assumes a steady state X_∞ , solution of the (stationary) CARE. Figure 2 depicts the difference between $X(t=100)$ and X_∞ , demonstrating that METD1 and both variants of METD2 converge to the stationary solution at their respective order.

4.3 Turbulent fluctuations of Atmospheric Jets

To demonstrate the effectiveness of the METD algorithm, we next want to consider an example involving partial differential equations (PDEs), which results in a larger number of degrees of freedom when the spatial directions are discretized. We are considering geostrophic turbulence in the atmosphere, for example in large gaseous planets, for simplicity modeled as a 2D reduction of the planetary atmosphere in a single layer. A simple model for atmospheric flow on a rotating planet is given by the 2-dimensional, stochastically forced, quasi-geostrophic equation in the β -plane [29]: For a periodic domain $(x, y) \in \mathbb{T}_L^2 = [0, L]^2$, the wind velocity vector field $\vec{v} = (u, v) : \mathbb{T}_L^2 \mapsto \mathbb{R}^2$, and its corresponding vorticity, $\omega = \nabla^\perp \vec{v}$, evolves according to

$$\partial_t \omega + \vec{v} \cdot \nabla \omega + \beta v = -\lambda \omega - \nu (-\Delta)^p \omega + \sqrt{\gamma} \eta. \quad (19)$$

Here, the stream function $\psi : \mathbb{T}_L^2 \rightarrow \mathbb{R}$ relates to the velocity via $\vec{v} = e_z \times \nabla \psi$, and the vorticity fulfills $\omega = \Delta \psi$. Equation (19) includes a linear Ekman-damping term with friction coefficient λ , and hyperviscosity of order p with viscosity coefficient ν . The stochastic noise η scales with amplitude γ , and has covariance

$$\mathbb{E}[\eta(x, y, t) \eta(x', y', t')] = \delta(t - t') \chi(|(x, y) - (x', y')|), \quad (20)$$

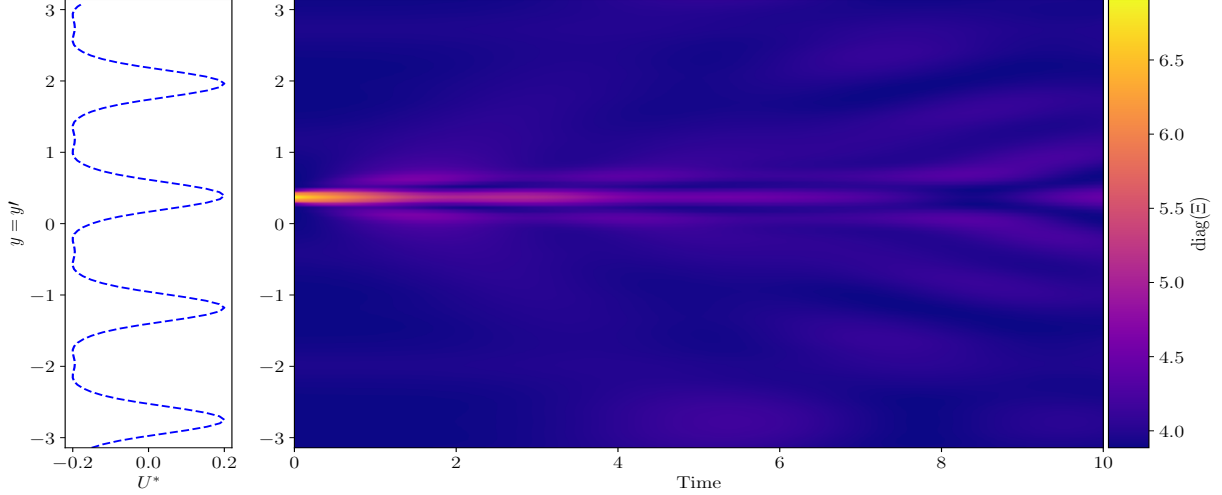


Figure 3: Perturbation on top of zonal jets decaying to a fixed point through the evolution of fluctuations via the differential Lyapunov equation (23). The plot on the left shows the stable zonal jet profile U^* with the stable 4 jet configuration. Integrated using the METD2 scheme.

i.e. the noise is homogeneous and isotropic. Lastly, the β -term models the Coriolis forces due to the planet's rotation, and determines the x -direction to be the zonal direction.

For a wide range of parameters, equation (19) exhibits the formation of large-scale coherent structures in the form of atmospheric jets, comparable to those observed on Jupiter or Saturn, and to a lesser degree Earth's jet stream. Defining as $U(y) = \bar{u}(y) = \int u(x, y) dx$ the zonal velocity average, we can obtain an evolution equation for the zonal velocity, depending on higher-order turbulent vorticity fluctuations, by making the ansatz $u(x, y) \leftarrow U(y) + \sqrt{\alpha}u(x, y)$ and $v(x, y) \leftarrow \sqrt{\alpha}v(x, y)$ [30, 31]. Considering $\Xi(x, y, x', y') = \mathbb{E}[\omega(x, y)\omega(x', y')]$, the covariance of the two-point correlation function of vorticity fluctuations, the system we obtain is

$$\begin{cases} \partial_t U &= -\alpha \bar{v} \bar{\omega} - \alpha U + \nu \partial_y^{2p} U \\ \partial_t \Xi &= -(\Gamma(U) \Xi + \Xi \Gamma(U)^\dagger) + 2C, \end{cases} \quad (21)$$

where $(\cdot)^\dagger$ denotes the adjoint and C is the spatial correlation function of the forcing, $\mathbb{E}[\eta(x, y, t)\eta(x', y', t')] = \delta(t-t')C(x, y, x', y')$. In this approach, the nonlinear self-interaction of the fluctuation field is neglected, and we define

$$\Gamma(U) := U \partial_x + (\partial_y^2 U - \beta) \partial_x \Delta^{-1} + \alpha + \nu (-\Delta)^p. \quad (22)$$

Note that this system is commonly referred to as the second-order cumulant expansion (CE2) system [19, 32, 33]. It relates the slow evolution of atmospheric jets under the influence of fast turbulent fluctuations through the Reynolds stress [34, 35]. We have a time scale separation in this system between the slow varying zonal jets and the fast turbulent fluctuations.

By considering stable jet configurations $U^*(u)$, with $\partial_t U^* = 0$, perturbations of the turbulent fluctuations evolve via the Lyapunov system

$$\partial_t \Xi = -(\Gamma(U^*) \Xi + \Xi \Gamma(U^*)^\dagger) + 2C. \quad (23)$$

In this example, we discretize our problem into a grid of size $N_x \times N_y$, and use pseudo-spectral methods to solve our system. We choose $N_x = 64$ and $N_y = 128$, resulting in a total of $n = N_x N_y = 8192$, so that $\Xi \in \mathbb{R}^{8192 \times 8192}$ to be solved by the METD scheme.

Implementation details. Our parameters are $\beta = 5$, $\alpha = 1 \times 10^{-3}$, $\nu = 1 \times 10^{-6}$ and $p = 4$. We consider the y -direction in real space and take the x -direction in Fourier space. This allows us to decouple each Fourier mode and integrate equation (23) for each Fourier mode independently.

The particular difficulty of this problem is the fact that the Γ -operator includes a hyper-viscosity term which is the Laplacian operator (Δ) raised to the power p . This term dissipates fluctuations on the smallest scales (or highest modes) in our system which increases the range of resolved scales. High orders of p are often used in fluid-dynamics applications to effectively dampen fine scales of fluctuations without influencing larger scales, resulting in a broad band of physically meaningful length-scales not affected by viscosity. On the other hand, high orders of p result in extremely harsh Courant–Friedrichs–Lewy (CFL) conditions, which for naive explicit solvers would require an extremely small time step. METD allows us to retain numerical stability even for very large time steps in this example (such as $\Delta t = 0.5$), due to the exact treatment of the linear Γ -operator. This improves integration performance of the system immensely.

As a concrete test case, we start the integration with an initial perturbation localized to a specific latitude, and can thus observe the propagation of the (variance of the) disturbance on the background of the atmospheric jet. The perturbation we choose is a simple Gaussian field centered at $\Xi_{y=y'}$ on a jet and we study the decay of this perturbation through the dynamic Lyapunov equation (23). Figure 3 shows the evolution of the perturbed diagonal of the correlation function. This example demonstrates the applicability of our matrix-ETD integration schemes in a complex setting.

4.4 Comparison with vectorized methods

Instead of considering a matrix version of ETD we can of course vectorize the system and implement traditional ETD. While this immediately solves all issues arising from non-commutativity, an immediate consequence of this vectorization is that the resulting ODEs are extremely large. To be more precise, if we were to vectorize (1), we would have the system

$$\dot{\hat{Q}} = \mathcal{L} \hat{Q} + \mathcal{N}(\hat{Q}), \quad (24)$$

for $\hat{Q} \in \mathbb{R}^{n^2}$, where $\mathcal{L} \in \mathbb{R}^{n^2 \times n^2}$ is the linear operator containing left- and right-multiplication of L and R , and $\mathcal{N} \in \mathbb{R}^{n^2}$ is potentially inhomogeneous. Applying ETD to this equation would require a matrix exponential of the linear operator \mathcal{L} which is much larger than the original linear operators in (1). Since the matrix exponential has time complexity $\mathcal{O}(n^3)$, this makes vectorization unattractive for large matrix-valued ODE's.

4.5 Extensions with Neural ODE's

4.5.1 Non-commuting L and R , Baker-Campbell-Hausdorff Formula

We can extend the system (1) to non-commuting L and R ($[L, R] \neq 0$). This makes computing the integral in (2) more complicated as we cannot simply split the exponential of a sum of matrices into products of matrix exponentials, $e^L e^R \neq e^{L+R}$. Let \mathcal{A} be a unital associative algebra over a field \mathbb{F} with characteristic zero and $L, R \in \mathcal{A}$. If $[L, R] = 0$, then we obtain the common relation

$$\begin{aligned} e^{L+R} &= \sum_{j=0}^{\infty} \frac{(L+R)^j}{j!} = \sum_{j=0}^{\infty} \sum_{k=0}^j \binom{j}{k} \frac{L^k R^{j-k}}{j!} \\ &= \sum_{j=0}^{\infty} \sum_{k=0}^j \frac{L^k R^{j-k}}{k!(j-k)!} \\ &= \sum_{s,t=0}^{\infty} \frac{L^s R^t}{s!t!} = e^L e^R. \end{aligned}$$

However, if $[L, R] \neq 0$, we can assume that there exists a $Z \in \mathcal{A}$ such that $e^L e^R = e^Z$ where $Z = \log(e^L e^R)$. Considering the power expansion of the logarithm function

$$\log(M) = \sum_{k=1}^{\infty} \frac{(-1)^{k-1}}{k} (M-1)^k,$$

we can substitute M by $e^L e^R$ and obtain the Lie series called the Baker-Campbell-Hausdorff (BCH) series

$$\begin{aligned} Z(L, R) &= \log(e^L e^R) \\ &= \sum_{k=1}^{\infty} \frac{(-1)^{k-1}}{k} \left(\sum_{s,t=0}^{\infty} \frac{L^s R^t}{s!t!} - 1 \right)^k \\ &= \sum_{k=1}^{\infty} \frac{(-1)^{k-1}}{k} \sum_{s_1+t_1>0} \dots \sum_{s_k+t_k>0} \frac{L^{s_1} R^{t_1} \dots L^{s_k} R^{t_k}}{s_1!t_1! \dots s_k!t_k!} \\ &= L + R + \frac{1}{2}[L, R] + \frac{1}{12}([L, [L, R]] - [R, [L, R]]) + \dots, \end{aligned}$$

where the “...” includes higher-order commutator nestings of L and R . Clearly if L and R commute, then the BCH series truncates after the first terms leaving $Z(L, R) = L + R$. In general, the BCH series cannot be truncated at low order to obtain an approximation of $Z(L, R)$. We therefore, rely on the following theorem:

Theorem 1 ([36]) *Suppose $L, R \in \mathcal{B}$ where \mathcal{B} is a Banach algebra over \mathbb{R} or \mathbb{C} . If $\|L\| + \|R\| < \log(2)/2$, then the Baker-Campbell-Hausdorff series converges absolutely to $\log(e^L e^R)$.*

Non-commutativity of L and R means that we cannot obtain the nice integrals in (5) and instead our integral in (2) has to be written as

$$\begin{aligned} \int_0^{\Delta t} e^{(\Delta t - \tau)L} N(t + \tau) e^{(\Delta t - \tau)R} d\tau &= \int_0^{\Delta t} e^{(\Delta t - \tau)(Z(L, R))} N(t + \tau) d\tau \\ &+ \int_0^{\Delta t} e^{(\Delta t - \tau)L} [N(t + \tau), e^{(\Delta t - \tau)R}] d\tau, \end{aligned} \quad (25)$$

where the series $Z(L, R)$ replaces the sum $L + R$. This means that the first order scheme will be

$$Q_{n+1} = \varphi_0(\Delta t L) Q_n \varphi_0(\Delta t R) + \varphi_1[\Delta t Z(L, R)] N(Q_n, t_n)$$

for non-commuting L and R , where still

$$\varphi_0(\Delta t A) = e^{\Delta t A}, \quad \varphi_1(\Delta t A) = (\Delta t A)^{-1} [e^{\Delta t A} - \mathbb{1}].$$

The same approach holds true for the higher order schemes.

4.5.2 Differential Sylvester equation

We can generalize the METD scheme further to non-square problems. These systems are of the form shown in (1) except we now have $L \in \mathbb{R}^{m \times m}$, $R \in \mathbb{R}^{n \times n}$ with $Q, N \in \mathbb{R}^{m \times n}$ where $m > n$, so the matrices Q and $N(Q)$ are non-square. For the special case of N constant, this system is known as the differential Sylvester equation and has a unique solution when the spectra of L and $-R$ are disjoint [13]. The differential Lyapunov equation is a symmetric case ($L = R^T$) of the differential Sylvester equation. We cannot use the METD schemes presented in earlier sections without modification since we cannot consider the commutativity of matrices of different dimensions.

We can augment the operators such that we have a square system that considers all degrees of freedom. A valid augmentation is zero-padding the matrices to match the dimension of the largest matrix in the system. We would then have an augmented system

$$\dot{\tilde{Q}} = L \tilde{Q} + \tilde{Q} \tilde{R} + \tilde{N}, \tag{26}$$

where $\tilde{Q}, \tilde{N} \in \mathbb{R}^{m \times m}$ are zero-padded matrices with $m - n$ zero columns right-concatenated to the original Q and N matrices and $\tilde{R} = R \oplus 0_{m,m}$ where \oplus is the matrix direct sum. With this augmentation, we can consider the commutator $[\tilde{N}, \tilde{R}]$ which allows us to approximate the integral in (2). We only need to zero-pad when approximating the integral in (2) and can easily remove the columns of zeros in our solution since the padded degrees of freedom do not ever interact with the original degrees of freedom. Of course, this strategy generalizes to an arbitrary non-square nonlinearity $N(Q)$.

Regarding the concrete implementation, we can use properties of the matrix exponential such that we do not ever compute the matrix exponential of the padded matrix \tilde{R} explicitly. The matrix exponential of a block zero matrix is the block identity matrix which means we can compute the matrix exponential of the smaller R matrix and pad it with an identity matrix to avoid computing the matrix exponential of the larger \tilde{R} (proof given in lemma 3). All matrix multiplications can be carried out with the original matrices since the padded degrees of freedom do not interact. These properties allow us to implement METD for the case $m > n$ with fewer operations than naively implementing METD for the augmented system (26).

4.5.3 Continuous Graph Neural Networks

The following example will make use of the generalizations discussed in the previous sections. Let us define a simple graph $G := (V, E)$ where V is the set of vertices and $E \subseteq V \times V$ is

the set of edges between vertices. Following Xhonneux et al. [4], we can represent the graph structure using a (regularized) adjacency matrix

$$\tilde{A} =: \frac{\alpha}{2} \left(\mathbf{1} + D^{-\frac{1}{2}} A D^{-\frac{1}{2}} \right), \quad (27)$$

where $\alpha \in (0, 1)$ is a hyperparameter, $A \in \mathbb{R}^{|V| \times |V|}$ is the typical adjacency matrix and $D_{ii} = \sum_j A_{ij}$ is the degree matrix. This modification, first introduced by Kipf et al. [37], stabilizes graph learning by shifting the eigenvalues of the adjacency matrix to the interval $[0, \alpha]$.

In addition to the adjacency matrix, we have a finite set of features F , and a node feature matrix $X \in \mathbb{R}^{|V| \times |F|}$ with $|F|$ being the number of node features. Our objective is to then learn a matrix of node representations $Q \in \mathbb{R}^{|V| \times d}$ where d is the dimension of the representation and the i -th row of Q corresponds to the representation of the i -th node.

Graph neural networks (GNNs) [37, 38, 39] provide a robust framework for learning node representations by processing complex, non-Euclidean graph data. GNNs typically model the discrete dynamics of node representations using multiple propagation layers. In each layer, every node’s representation is updated based on the representations of its neighboring nodes (message passing).

However, existing GNNs (e.g. GCN [37], GraphSage [39], GATs [38]) have been shown to suffer from a phenomenon called over-smoothing [40]. Over-smoothing occurs when node representations in a graph become increasingly similar through multiple layers of message passing, leading to a loss of discriminative power and ultimately, poor performance. An interesting model by Xhonneux et al. [4] tries to mitigate the over-smoothing problem by taking inspiration from Neural ODE’s [41] and adapting the discrete dynamics to a continuous space. We, therefore, have a continuous dynamical system to model the continuous dynamics on node representations. Moreover, it has been shown that this approach does not experience the over-smoothing problem, because the model converges to a meaningful representation as $t \rightarrow \infty$ given by a fixed point [4, 42, 43].

The Continuous Graph Neural Network (CGNN) [4] architecture consists of three main components. First, a neural encoder projects each node into a latent space based on its features, resulting in $E = \mathcal{E}(X)$, where \mathcal{E} represents the encoder. Next, E is used as the initial value $H(0)$, and an ODE is designed to define the continuous dynamics of node representations, effectively modeling long-term dependencies between nodes. Finally, the node representations at the end time t_n (i.e., $H(t_n)$) are used for downstream tasks through a decoder \mathcal{D} , yielding a node-label matrix $Y = \mathcal{D}(H(t_n))$.

One example of an ODE to model the continuous dynamics of node representations is

$$\dot{Q}(t) = (\tilde{A} - \mathbf{1})Q(t) + Q(t)(W - \mathbf{1}) + E, \quad (28)$$

where $W \in \mathbb{R}^{d \times d}$ is a weight matrix. This is a differential Sylvester equation where the left and right operators govern system dynamics with the inhomogeneity being the initial input E from the encoder network. This system includes both extensions mentioned earlier: non-commuting operators and a non-square system. We integrate this system using our matrix ETD solver and show that it can solve complex high-dimensional Sylvester systems.

Datasets. We study our schemes using the three most popular citation networks in the literature, Cora [44], Citeseer [45] and Pubmed [46]. We make use of random weight initializations of fixed splits of these datasets and show a direct comparison in Table 1.

Table 1: Node classification test accuracy and std for 20 random initializations using the Planetoid train-val-test splits. Bold results indicate the highest test accuracy for its respective dataset. *Results obtained by running author’s original code with parameters given in their paper.

PLANETOID SPLITS	CORA	CiteSeer	PubMed
#NODES	2,708	3,327	18,717
#EDGES	5,278	4,676	44,327
#CLASSES	6	7	3
Dopri5*	81.8 \pm 0.7	68.1 \pm 1.2	80.3 \pm 0.3
Explicit AB	32.0 \pm 1.9	30.1 \pm 1.8	31.1 \pm 1.9
Implicit AM	82.3 \pm 0.6	69.0 \pm 0.7	80.5 \pm 0.4
METD1_BCH1	80.4 \pm 1.4	67.3 \pm 1.0	80.0 \pm 0.5
METD1_BCH2	82.8 \pm 0.5	67.5 \pm 1.2	80.4 \pm 0.7
METD1_BCH3	83.0 \pm 0.5	68.9 \pm 1.1	80.9 \pm 0.6
METD2_BCH1	80.8 \pm 1.4	67.9 \pm 1.1	80.3 \pm 0.8
METD2_BCH2	83.0 \pm 0.6	68.0 \pm 1.0	80.5 \pm 0.6
METD2_BCH3	82.9 \pm 0.5	69.1 \pm 0.8	80.8 \pm 0.5

Implementation details. All schemes in this example have been implemented in PyTorch [47] using torchdiffeq [41] and PyTorch geometric [48]. The hyperparameters from Xhonneux et al. [4] were used for all schemes. We do, however, use Theorem 1 to make sure our BCH series is convergent by varying the hyperparameter α . To ensure non-singularity of $Z(L, R)$ in our schemes during training, we add some regularization to $Z(L, R)$ such that we do not have any null eigenvalues. We also use the ANODE augmentation scheme [49] to stabilize training.

To demonstrate that our METD schemes work on differential Sylvester equations, we solve the ODE (28) and show the test accuracy results for the METD schemes compared to the default in most packages which is the adaptive Runge-Kutta 4(5) Dormand & Price (Dopri5) scheme which we take as the baseline. We also compare our schemes to the explicit 4th order Adams–Bashforth (Explicit AB) and the implicit 4th order Adams–Moulton (Implicit AM) schemes. Table 1 summarises that we achieve comparable results to the original CGNN implementation using the Dopri5 solver which shows that the extended METD schemes work well with differential Sylvester equations. The nomenclature of METD $_j$ _BCH $_n$ for positive integers j and n signify the order j of the METD scheme as well as the BCH series truncation order n .

The explicit AB scheme is unstable for all step sizes except for very small time steps ($\Delta t = 0.005$) which makes using this solver impractical since a single epoch takes a significant amount of time. The implicit AM scheme is stable for all step sizes except large ones ($\Delta t = 10$) however, with a large step size, the implicit equations can become more difficult to solve. Table 2 shows a comparison of running times per epoch for some schemes. We see that the METD1_BCH3 scheme is faster as well as just as accurate (test accuracy wise from table 1) as the implicit AM scheme.

Note that we are not aiming to outperform the benchmark, but rather to show that our

Table 2: Average running times per epoch for various fixed time step schemes on the Cora dataset. Out of the step sizes tried for the explicit AB scheme, only $\Delta t = 0.005$ was stable. The implicit AM scheme is the most expensive time wise per epoch compared to other schemes. The METD1_BCH3 scheme has the lowest running time.

FIXED TIME STEP SCHEMES	Explicit AB ($\Delta t = 0.005$)	Implicit AM ($\Delta t = 0.01$)	METD1_BCH3 ($\Delta t = 0.01$)
Average time per epoch (s)	9.2	19.2	2.9

schemes can integrate these complex systems and perform just as well as state-of-the-art integrators while taking less time.

In some cases, we do actually outperform the original implementation. For example, the METD1_BCH3 scheme outperforms the original implementation for all the benchmark datasets tested. We also observed that using METD, we can choose the time step to be significantly larger than when using Runge-Kutta methods. With just 3 layers, we can achieve comparable accuracy to the Runge-Kutta CGNN which has potentially hundreds of layers depending on the stability.

5 Conclusion

We have extended the ETD numerical method to matrix differential equations which have a stiff linear part using elements from Lie algebra. A significant advantage of these schemes stems from the fact that the linear part is solved exactly which makes these stiff problems tractable from a numerical point of view. Integrating matrix-valued dynamical systems using vectorization and classic ETD is prohibitively expensive for large systems, while METD schemes translate the ideas of ETD onto matrix evolution equations without a large increase in computational effort.

In terms of algorithms, we derived first and second-order METD multi-step schemes as well as a Runge-Kutta form of second order which does not require an initialization. These METD schemes enjoy desirable stability properties and can be applied to a variety of problems including matrix-ODE and PDE systems.

We have carried out a number of numerical tests for the METD schemes. We have confirmed the global truncation error for the first, second and Runge-Kutta schemes on differential Lyapunov and Ricatti equations. In these examples, we only consider the case of commuting left and right operators which is typical when arriving at the equations from stochastic systems. We showed how these methods all easy integration of a severely stiff system that models jet formation in atmospheres of large planets which would usually require an extremely small time step.

Finally, we considered a continuous GNN where a Sylvester equation replaces the discrete layers typically seen in neural networks. In order to apply the developed methods for this problem, it was necessary to extend the METD scheme to non-commuting operators with a non-square system and to relax some of the assumptions about the involved commutators. We reported test accuracies for three benchmark datasets and compared these to the default

adaptive Runge-Kutta 4(5) Dormand & Price scheme as well as other fixed time step schemes showing comparable accuracy. We show a significant speedup compared to other fixed time step schemes. We also showed that by using just one integration step (i.e. one layer) we achieve accuracies comparable to a model with a thousand layers.

A Useful Lemmas and derivations

Lemma 1 *Let A be an arbitrary matrix $A \in \mathbb{C}^{n \times n}$ and $t \in \mathbb{R}$, then the commutator $[A, e^{-tA}] = 0$.*

Proof.

We have that $[A, e^{-tA}] = Ae^{-tA} - e^{-tA}A$ and expanding both matrix exponentials as a power series gives us

$$\begin{aligned} Ae^{-tA} - e^{-tA}A &= A \left[\sum_{n=0}^{\infty} \frac{(-t)^n}{n!} (A)^n \right] - \left[\sum_{n=0}^{\infty} \frac{(-t)^n}{n!} (A)^n \right] A \\ &= \sum_{n=0}^{\infty} \frac{(-t)^n}{n!} (A)^{n+1} - \sum_{n=0}^{\infty} \frac{(-t)^n}{n!} (A)^{n+1} \\ &= 0. \end{aligned}$$

□

A.1 Derivation of METD1

Take the first order approximation of the integral of the non-linear term

$$\int_0^{\Delta t} e^{(\Delta t - \tau)(L+R)} d\tau N(t_n),$$

and set $A =: L + R$ with a substitution $s = \Delta t - \tau$. Changing the limits of integration with the substitution gives us the integral with solution

$$\begin{aligned} \int_0^{\Delta t} e^{sA} ds N(t_n) &= [(e^{\Delta t A} - \mathbf{1}) A^{-1}] N(t_n) \\ &= [(L + R)^{-1} (e^{\Delta t (L+R)} - \mathbf{1})] N(t_n) \end{aligned}$$

with $(e^{\Delta t A} - \mathbf{1})$ and A^{-1} commuting from lemma 1.

Lemma 2 *Let $L \in \mathbb{C}^{n \times n}$ then $\int_0^t se^{sL} ds = \mathcal{O}(t^2)$.*

Proof. By integrating, we have

$$\begin{aligned}
\int_0^t s e^{sL} ds &= L^{-2} (t e^{tL} L - e^{tL} + \mathbf{1}) \\
&= L^{-2} \left(t \sum_{n=0}^{\infty} \frac{t^n}{n!} L^{n+1} - \sum_{n=0}^{\infty} \frac{t^n}{n!} L^n + \mathbf{1} \right) \\
&= L^{-2} \left([tL + t^2 L^2 + \frac{t^3}{2} L^3 + \dots] - [\mathbf{1} + tL + \frac{t^2}{2} L^2 + \dots] + \mathbf{1} \right) \\
&= L^{-2} \left(\frac{t^2}{2} + \mathcal{O}(t^3) \right) \\
&= \mathcal{O}(t^2)
\end{aligned}$$

□

A.2 Derivation of METD2

By setting $\xi_n = (N_n - N_{n-1})/\Delta t$, we can arrive at the following integrals

$$\begin{aligned}
\int_0^{\Delta t} e^{(\Delta t - \tau)L} N(t_n + \tau) e^{(\Delta t - \tau)R} d\tau &= \int_0^{\Delta t} e^{(\Delta t - \tau)(L+R)} N(t_n + \tau) d\tau \\
&\quad + \int_0^{\Delta t} (\Delta t - \tau) e^{(\Delta t - \tau)L} [N(t_n + \tau), R] d\tau + \mathcal{O}(\Delta t^3) \\
&= \int_0^{\Delta t} e^{(\Delta t - \tau)(L+R)} (N_n + \tau \xi_n) d\tau \\
&\quad + \int_0^{\Delta t} (\Delta t - \tau) e^{(\Delta t - \tau)L} [(N_n + \tau \xi_n), R] d\tau \\
&= I_n + C_n
\end{aligned}$$

where we are solving both integrals separately for simplicity.

$$\begin{aligned}
I_n &= \int_0^{\Delta t} e^{(\Delta t - \tau)(L+R)} d\tau N_n + \int_0^{\Delta t} e^{(\Delta t - \tau)(L+R)} \tau d\tau \xi_n \\
&= (L + R)^{-1} (e^{\Delta t(L+R)} - \mathbf{1}) N_n + (L + R)^{-2} (e^{\Delta t(L+R)} - \Delta t(L + R) - \mathbf{1}) \xi_n
\end{aligned}$$

and

$$\begin{aligned}
C_n &= \int_0^{\Delta t} (\Delta t - \tau) e^{(\Delta t - \tau)L} [(N_n + \tau \xi_n), R] d\tau \\
&= \int_0^{\Delta t} (\Delta t - \tau) e^{(\Delta t - \tau)L} d\tau [N_n, R] + \int_0^{\Delta t} \tau (\Delta t - \tau) e^{(\Delta t - \tau)L} d\tau [\xi_n, R] \\
&= L^{-2} (\Delta t e^{\Delta t L} L - e^{\Delta t L} + \mathbf{1}) [N_n, R] + L^{-3} (\Delta t L + \Delta t e^{\Delta t L} L - 2e^{\Delta t L} + 2\mathbf{1}) [\xi_n, R].
\end{aligned}$$

Lemma 3 Let $A \in \mathbb{C}^{n \times n}$ and $\tilde{A} \in \mathbb{C}^{m \times m}$ where $m > n$ with A zero-padded to form \tilde{A} i.e. $\tilde{A} = \begin{bmatrix} A & 0_{n \times (m-n)} \\ 0_{(m-n) \times n} & 0_{(m-n)} \end{bmatrix}$. The matrix exponential of \tilde{A} will then be $e^{\tilde{A}} = \begin{bmatrix} e^A & 0 \\ 0 & \mathbb{I}_{(m-n)} \end{bmatrix}$, i.e. e^A padded by an identity matrix $\mathbb{I}_{(m-n)}$.

Proof. Using the definition of the matrix exponential,

$$\begin{aligned}
e^{\tilde{A}} &= \sum_{k=0}^{\infty} \frac{1}{k!} (\tilde{A})^k \\
&= \begin{bmatrix} \mathbb{I}_n & 0 \\ 0 & \mathbb{I}_{(m-n)} \end{bmatrix} + \begin{bmatrix} A & 0_{n \times (m-n)} \\ 0_{(m-n) \times n} & 0_{(m-n)} \end{bmatrix} + \frac{1}{2!} \begin{bmatrix} A^2 & 0_{n \times (m-n)} \\ 0_{(m-n) \times n} & 0_{(m-n)} \end{bmatrix} + \dots \\
&= \begin{bmatrix} \mathbb{I}_n + A + \frac{1}{2!}A^2 + \dots & 0 \\ 0 & \mathbb{I}_{(m-n)} \end{bmatrix} \\
&= \begin{bmatrix} e^A & 0 \\ 0 & \mathbb{I}_{(m-n)} \end{bmatrix}.
\end{aligned}$$

□

References

- [1] F. Amato, R. Ambrosino, M. Ariola, C. Cosentino, G. De Tommasi, et al., Finite-time stability and control, Vol. 453, Springer, 2014.
- [2] M. Athans, P. L. Falb, Optimal control: an introduction to the theory and its applications, Courier Corporation, 2013.
- [3] S. Gugercin, A. C. Antoulas, C. Beattie, H₂ model reduction for large-scale linear dynamical systems, SIAM journal on matrix analysis and applications 30 (2) (2008) 609–638.
- [4] L.-P. Xhonneux, M. Qu, J. Tang, Continuous Graph Neural Networks, in: H. D. III, A. Singh (Eds.), Proceedings of the 37th International Conference on Machine Learning, Vol. 119 of Proceedings of Machine Learning Research, PMLR, 2020, pp. 10432–10441.
- [5] R. E. Kalman, R. S. Bucy, New Results in Linear Filtering and Prediction Theory, Journal of Basic Engineering 83 (1) (1961) 95–108.
- [6] D. Simon, Optimal state estimation: Kalman, H infinity, and nonlinear approaches, John Wiley & Sons, 2006.
- [7] J. Y.-K. Cho, L. M. Polvani, The emergence of jets and vortices in freely evolving, shallow-water turbulence on a sphere, Physics of Fluids 8 (6) (1996) 1531–1552.
- [8] S. D. Danilov, D. Gurarie, Quasi-two-dimensional turbulence, Physics-Uspekhi 43 (9) (2000) 863.
- [9] D. Higham, L. Trefethen, Stiffness of ODEs, BIT Numerical Mathematics 33 (2) (1993) 285–303.
- [10] J. M. Prusa, P. K. Smolarkiewicz, A. A. Wyszogrodzki, Eulag, a computational model for multiscale flows, Computers & Fluids 37 (9) (2008) 1193–1207.

- [11] P. Benner, H. Mena, BDF methods for large-scale differential Riccati equations, *Proc. of Mathematical Theory of Network and Systems, MTNS 2004* (2004) 10.
- [12] M. Köhler, N. Lang, J. Saak, Solving Differential Matrix Equations using Parareal: Parareal for DMEs, *PAMM* 16 (2016) 847–848.
- [13] M. Behr, P. Benner, J. Heiland, Solution formulas for differential Sylvester and Lyapunov equations, *Calcolo* 56 (12 2019).
- [14] A. Koskela, H. Mena, A Structure Preserving Krylov Subspace Method for Large Scale Differential Riccati Equations, 2017.
- [15] D. Li, X. Zhang, R. Liu, Exponential integrators for large-scale stiff Riccati differential equations, *Journal of Computational and Applied Mathematics* 389 (2021) 113360.
- [16] S. M. Cox, P. C. Matthews, Exponential Time Differencing for Stiff Systems, *Journal of Comp. Phys.* 174 (2002) 430–455.
- [17] A. Friedli, Generalized Runge-Kutta Methods for the Solution of Stiff Differential Equations, *Numerical Treatment of Differential Equations*, R. Burlirsch, R. Grigorieff, and J. Schröder, eds 631 (1978) 35–50.
- [18] P. Petropoulos, Analysis of exponential time-differencing for FDTD in lossy dielectrics, *IEEE Transactions on Antennas and Propagation* 45 (6) (1997) 1054–1057.
- [19] K. Srinivasan, W. R. Young, Zonostrophic Instability, *Journal of the Atmospheric Sciences* 69 (5) (2012) 1633 – 1656.
- [20] V. Bratanov, F. Jenko, E. Frey, New class of turbulence in active fluids, *Proceedings of the National Academy of Sciences* 112 (2015) 201509304.
- [21] U. Frisch, S. Kurien, R. Pandit, W. Pauls, S. S. Ray, A. Wirth, J.-Z. Zhu, Hyperviscosity, Galerkin truncation, and bottlenecks in turbulence, *Physical review letters* 101 (14) (2008) 144501.
- [22] L. Ju, J. Zhang, L. Zhu, Q. Du, Fast explicit integration factor methods for semilinear parabolic equations, *Journal of Scientific Computing* 62 (2) (2015) 431–455.
- [23] B. V. Minchev, W. M. Wright, A review of exponential integrators for first order semi-linear problems, 2005.
- [24] V. T. Luan, A. Ostermann, Explicit exponential Runge–Kutta methods of high order for parabolic problems, *Journal of Computational and Applied Mathematics* 256 (2014) 168–179.
- [25] M. Hochbruck, A. Ostermann, Exponential integrators, *Acta Numerica* 19 (2010) 209–286.

- [26] J. Niesen, W. M. Wright, Algorithm 919: A Krylov Subspace Algorithm for Evaluating the φ -Functions Appearing in Exponential Integrators, *ACM Transactions on Mathematical Software* 38 (3) (2012) 1–19.
- [27] A. H. Al-Mohy, N. J. Higham, A new scaling and squaring algorithm for the matrix exponential, *SIAM Journal on Matrix Analysis and Applications* 31 (3) (2009) 970 – 989.
- [28] P. Lancaster, L. Rodman, *Algebraic Riccati Equations*, Oxford Science Publications, 1995.
- [29] S. Danilov, D. Gurarie, Scaling, spectra and zonal jets in beta-plane turbulence, *Physics of Fluids* 16 (7) (2004) 2592–2603.
- [30] F. Bouchet, C. Nardini, T. Tangarife, Kinetic Theory of Jet Dynamics in the Stochastic Barotropic and 2d Navier-Stokes Equations, *Journal of Statistical Physics* 153 (4) (2013) 572–625.
- [31] F. Bouchet, J. B. Marston, T. Tangarife, Fluctuations and large deviations of Reynolds stresses in zonal jet dynamics, *Physics of Fluids* 30 (1) (2018) 015110.
- [32] B. F. Farrell, P. J. Ioannou, Structural Stability of Turbulent Jets, *Journal of the Atmospheric Sciences* 60 (17) (2003) 2101 – 2118.
- [33] N. A. Bakas, P. J. Ioannou, Emergence of Large Scale Structure in Barotropic β -Plane Turbulence, *Phys. Rev. Lett.* 110 (2013) 224501.
- [34] F. Bouchet, E. Simonnet, Random Changes of Flow Topology in Two-Dimensional and Geophysical Turbulence, *Physical Review Letters* 102 (9) (2009) 094504.
- [35] F. Bouchet, J. Rolland, E. Simonnet, Rare Event Algorithm Links Transitions in Turbulent Flows with Activated Nucleations, *Physical Review Letters* 122 (7) (2019) 074502.
- [36] W. Rossmann, *Lie groups: an introduction through linear groups*, Vol. 5, Oxford University Press on Demand, 2006.
- [37] T. N. Kipf, M. Welling, Semi-Supervised Classification with Graph Convolutional Networks, in: *International Conference on Learning Representations (ICLR)*, 2017.
- [38] P. Velickovic, G. Cucurull, A. Casanova, A. Romero, P. Lio, Y. Bengio, et al., Graph attention networks, *stat* 1050 (20) (2017) 10–48550.
- [39] W. L. Hamilton, R. Ying, J. Leskovec, Inductive representation learning on large graphs, *Advances in neural information processing systems* 30 (2017).
- [40] Q. Li, Z. Han, X.-M. Wu, Deeper insights into graph convolutional networks for semi-supervised learning, in: *Proceedings of the AAAI conference on artificial intelligence*, Vol. 32, 2018.

- [41] R. T. Chen, Y. Rubanova, J. Bettencourt, D. K. Duvenaud, Neural Ordinary Differential Equations, *Advances in neural information processing systems* 31 (2018).
- [42] B. Chamberlain, J. Rowbottom, M. I. Gorinova, M. Bronstein, S. Webb, E. Rossi, Grand: Graph neural diffusion, in: *International Conference on Machine Learning*, PMLR, 2021, pp. 1407–1418.
- [43] M. Poli, S. Massaroli, J. Park, A. Yamashita, H. Asama, J. Park, Graph neural ordinary differential equations, *arXiv preprint arXiv:1911.07532* (2019).
- [44] A. K. McCallum, K. Nigam, J. Rennie, K. Seymore, Automating the construction of internet portals with machine learning, *Information Retrieval* 3 (2000) 127–163.
- [45] P. Sen, G. Namata, M. Bilgic, L. Getoor, B. Galligher, T. Eliassi-Rad, Collective classification in network data, *AI magazine* 29 (3) (2008) 93–93.
- [46] G. Namata, B. London, L. Getoor, B. Huang, U. Edu, Query-driven active surveying for collective classification, in: *10th international workshop on mining and learning with graphs*, Vol. 8, 2012, p. 1.
- [47] A. Paszke, S. Gross, F. Massa, A. Lerer, J. Bradbury, G. Chanan, T. Killeen, Z. Lin, N. Gimelshein, L. Antiga, et al., Pytorch: An imperative style, high-performance deep learning library, *Advances in neural information processing systems* 32 (2019).
- [48] M. Fey, J. E. Lenssen, Fast Graph Representation Learning with PyTorch Geometric, in: *ICLR Workshop on Representation Learning on Graphs and Manifolds*, 2019.
- [49] E. Dupont, A. Doucet, Y. W. Teh, Augmented Neural ODEs, in: H. Wallach, H. Larochelle, A. Beygelzimer, F. d'Alché-Buc, E. Fox, R. Garnett (Eds.), *Advances in Neural Information Processing Systems*, Vol. 32, Curran Associates, Inc., 2019.